Sartori Jeunon Gontijo, E., Monteiro, A.S.C., Tonello, P.S., Roeser, H.M.P., **Friese, K.**, Rosa, A.H. (2022):
Analyses of colloidal, truly dissolved, and DGT-labile metal species and phosphorus in mining area surrounded by tailing dams using self-organising maps
Chemosphere **303, Part 2** , art. 135003

http://dx.doi.org/10.1016/j.chemosphere.2022.135003

Analyses of colloidal, truly dissolved, and DGT-labile metal species and phosphorus in mining area surrounded by tailing dams using self-organising maps

Erik Sartori Jeunon Gontijo[a, *], Adnívia Santos Costa Monteiro[b], Paulo Sérgio Tonello[a], Hubert Mathias Peter Roeser[c], Kurt Friese[d], André Henrique Rosa[a, *]

a - Institute of Science and Technology, São Paulo State University (UNESP), Av. Três de Março, 511, Alto da Boa Vista – 18087-180 – Sorocaba- SP – Brazil, (+55 15) 3238-3414

b - Federal University of Sergipe (UFS), Campus São Cristóvão, Av. Marechal Rondon, s/n, Jardim Rosa Elze – 49100-000 – São Cristóvão- SE– Brazil

c - Federal University of Ouro Preto (UFOP), Campus Universitário, Morro do Cruzeiro 354000-000, Ouro Preto-MG, Brazil

d - Department of Lake Research, Helmholtz Centre for Environmental Research – UFZ, Brueckstr. 3a, 39114, Magdeburg, Germany

*corresponding authors: Erik S.J. Gontijo (sartori_jg@hotmail.com) and André H. Rosa (andre.rosa@unesp.br)

Highlights

- Values for trace metals and P were high before the Fundão dam failure in 2015
- P was mainly in the truly dissolved and DGT-labile fractions
- Increase of colloidal Fe reduced P in the DGT-labile fraction
- Most of total dissolved Cu was found in the colloidal fraction in Conceição River
- Differences between dry and wet seasons for Co, Fe and Ni detected by SO-Maps

Graphical Abstract

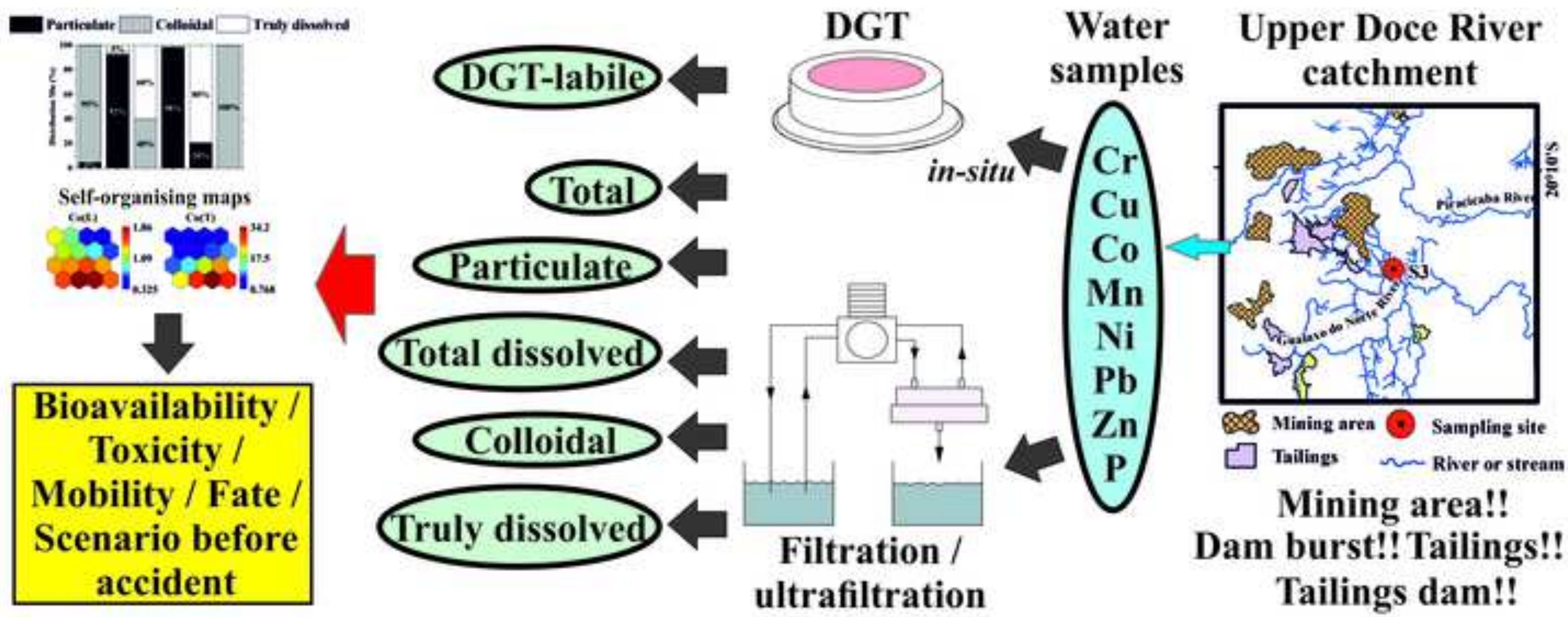

Analyses of colloidal, truly dissolved, and DGT-labile metal species and phosphorus in mining area surrounded by tailing dams using self-organising maps

Erik Sartori Jeunon Gontijo[a, *], Adnívia Santos Costa Monteiro[b], Paulo Sérgio Tonello[a], Hubert Mathias Peter Roeser[c], Kurt Friese[d], André Henrique Rosa[a, *]

a - Institute of Science and Technology, São Paulo State University (UNESP), Av. Três de Março, 511, Alto da Boa Vista – 18087-180 – Sorocaba- SP – Brazil, (+55 15) 3238-3414

b - Federal University of Sergipe (UFS), Campus São Cristóvão, Av. Marechal Rondon, s/n, Jardim Rosa Elze – 49100-000 – São Cristóvão- SE– Brazil

c - Federal University of Ouro Preto (UFOP), Campus Universitário, Morro do Cruzeiro 354000-000, Ouro Preto-MG, Brazil

d - Department of Lake Research, Helmholtz Centre for Environmental Research – UFZ, Brueckstr. 3a, 39114, Magdeburg, Germany

*corresponding authors: Erik S.J. Gontijo (sartori_jg@hotmail.com) and André H. Rosa (andre.rosa@unesp.br)

Abstract

The knowledge of size-distribution and lability of metals and nutrients in freshwater systems is important for estimation of the ecological effects of mining. However, it is still limited in several mining areas such as the Quadrilátero Ferrífero (Brazil) which was severely polluted by the collapse of the Fundão tailings dam in November 2015. In this study, results of an investigation from 2014 using a neural network named self-organising map (SO-Map) into the conditions of selected trace metals that are of particular importance to mining areas (Cr, Cu, Co, Mn, Ni, Pb, Zn) are presented. Additionally, P was considered by its high importance as a nutrient and sites later affected by the dam burst were also included by chance. Water samples were collected at six sites in dry and rainy seasons and filtered and ultrafiltered for determination of total dissolved (< 0.45 µm) and truly dissolved (< 1 kDa) fractions. Diffusive gradients in thin films (DGT) devices were deployed *in situ* for determination of the DGT-labile fraction. All data were analysed using SO-Map and Spearman's rank correlation. Phosphorus in the Carmo River occurred mainly in the truly dissolved and DGT-labile fractions. The higher amounts of this element in the river water (up to 263 µg L^{-1} of total P) might be related to untreated sewage discharge. Moreover, the concentrations of other trace metals (Mn, Cu, Co, Ni, Zn) were high, even under the "natural" conditions (before the dam failure) due to natural and anthropogenic factors such as local lithology and mining.

Keywords: size fractionation, diffusive gradients in thin films, ultrafiltration, Kohonen neural network, mining impacts

1. Introduction

The Quadrilátero Ferrífero is a well-known mineral province located in the state of Minas Gerais, in southeast of Brazil (Deschamps et al., 2002; Varcjao et al., 2011). The gold and iron mining has caused several negative impacts in this region, including soil erosion and contamination of water, sediments, and soils (Deschamps et al., 2002; Roeser and Roeser, 2010; Varcjao et al., 2011; Gontijo et al., 2016). The construction of several tailings dams for storing wastes from mining activities has also become problematic, particularly by leaking of mine wastes and the collapse of tailings dams (Rodrigues et al., 2014; Santamarina et al., 2019). The accident near the city of Mariana in November 2015 (collapse of the Fundão tailings dam) for instance released more than 40 million m^3 of mining waste into the Upper Doce River catchment (Carmo et al., 2017; Vergilio et al., 2020).

Since the behaviour and fate of metals and metalloids in rivers are dependent on their chemical form, it is of high interest to study size-distribution and lability of metals and nutrients in aquatic systems. Metals and nutrients may be adsorbed in suspended particles, incorporated in living organisms, complexed with organic or inorganic ligands, or appear as free (hydrated) ions. These different forms have different mobility, toxicity and bioavailability in the environment (Buffle, 1991). As a result, the sole determination of total and even total dissolved concentrations of a given element is not sufficient to predict its effects on aquatic systems (Morel, 1983).

An important approach that can be used to better investigate trace metal speciation and mobility of metals and metalloids is size fractionation of water samples. Filtration and ultrafiltration (UF) are examples of techniques generally used for fractionating a given element into particulate, total dissolved, colloidal, and truly dissolved fractions, according to the used operational definition (Singhal et al., 2006; Gontijo et al., 2017a). While the species in the particulate fraction have low mobility and bioavailability, species in the truly dissolved fraction are more mobile and potentially bioavailable (Allen and Hansen, 1996; Wen et al., 1997).

The technique of diffusive gradients in thin films (DGT) can be used complementarily to UF. It is able of detect *in situ* labile species (including free species and DGT-labile complexes) which may be more bioavailable in water systems (Forsberg et al., 2006; Tonello et al., 2007; Rougerie et al., 2021). DGT devices are deployed in aqueous environments where metal ions diffuse through a diffusive boundary layer, a gel layer and accumulate in the binding layer of the sampler. The concentration of the metals accumulated in the binding layer during the deployment time is then measured and used to calculate the metal flux through the gel layer and the amount of labile species in the water (Davison and Zhang, 1994). These labile species are basically the ones able to dissociate and reach equilibrium along the diffusion medium during the deployment time (van Leeuwen and Jansen, 2005; Garmo et al., 2006; Sans-Duñó et al., 2021). Then, DGT is considered a dynamic technique since it represents the flux of metal species to the device (van Leeuwen et al., 2005).

The investigation of water quality and metal fractions requires the measurement of many variables that generates a huge amount of data. The analysis of these data and the complex relationship among variables requires the use of exploratory tools with good visualisation capabilities (Çinar and Merdun, 2009; Gontijo et al., 2021). The self-organising map (SO-Map), also known as Kohonen neural network, is an example of such tools. It is a type of neural network used for clustering and visualisation that converts high-dimensional data in a low-dimensional space, typically a two-dimensional grid of nodes (neurons) forming a rectangular map (Vesanto, 1999; Kohonen, 2001; Brereton, 2012).

This investigation has the objective to determine the distribution Cr, Cu, Co, Mn, Ni, Pb, Zn and P in the fractions total, total dissolved, truly dissolved, and DGT-labile in samples from rivers and streams in an area impacted by iron and gold mining using SO-Map. Sampling was carried out before the collapse of the Fundão tailings dam and included sites in the affected area. In this sense, our study can be a basis of comparison for the assessment of the contaminating effect of the dam failure. The presence of several tailings dams in the catchment also requires continuous monitoring of truly dissolved and DGT-labile metal and nutrient species for mobility and toxicity prediction. This type of study is still scarce in such impacted areas and may contribute to understand the effect on mining activities on metal distribution, mobility, and lability.

2. Material and methods

2.1. Study site and sampling

Six sampling sites (S1, S3, S4, S6, S7 and S9, Fig. 1) were investigated in Upper Doce River catchment in rainy and dry season (February and October, respectively) of 2014. Conductivity (µS cm^{-1}), total dissolved solids (TDS, mg L^{-1}), pH and temperature (°C) were measured *in situ* using a multi-parameter probe Ultrameter II (Myron L Company).

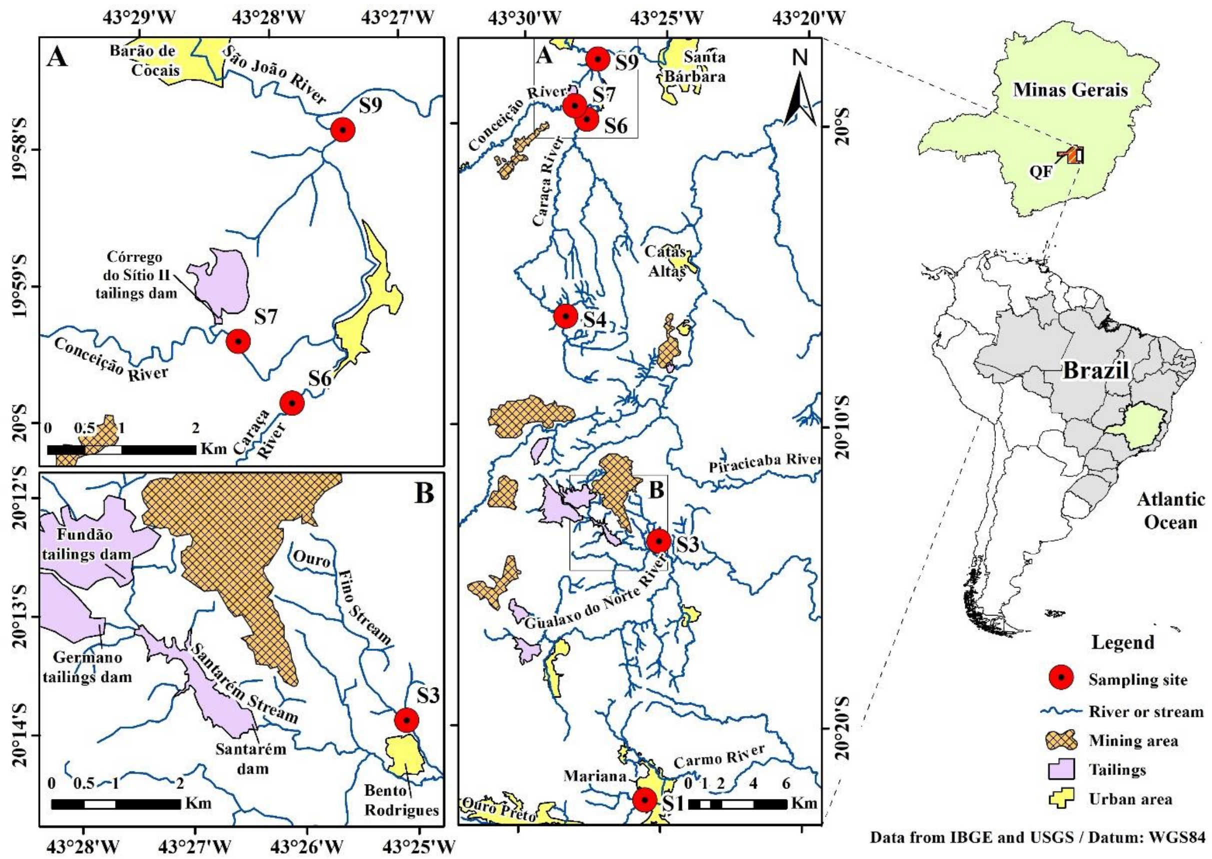

Fig. 1 Sampling sites (S1, S3, S4, S6, S7 and S9), mining areas and tailing dams in Upper Doce River catchment (in Quadrilátero Ferrífero, QF). Mining areas and tailing dams were delineated

using cloud-free Landsat 8 imagens taken from path 217 and row 74 on 11th October and 12th November 2015. The images were acquired from the U.S. Geological Survey (USGS) Earth Explorer webpage (https://earthexplorer.usgs.gov/, accessed in December 2020). All delineations were performed using the software ArcGis 10.5 (ESRI, USA).

The sampling sites were originally selected to investigate the As, Al and Fe distribution in rivers from Quadrilátero Ferrífero and the influence of dissolved organic matter on it (Gontijo et al., 2016). However, the presence of several dams in the Doce River catchment and the dam collapse in 2015 nearby the city of Mariana makes the investigation of the distribution of the trace metals Cr, Cu, Co, Mn, Ni, Pb and Zn in rivers near the dams remarkably important. The selected sites included analysis of DGT-labile species, except S3 which was selected because it was directly affected by the collapse of Fundão dam in 2015 [Fig. A.1, Appendix A, Supplementary Information (SI)]. While S1 and S3 are located in areas affected by the dam-burst disaster, sites S4, S6, S7 and S9 are located in rivers or streams surrounded by mining areas and tailings dams (Fig. 1) but were not affected by this disaster. Site S4 is a pristine area located in a private protected place; Private Reserve of the Natural Heritage, RPPN.

Freshwater samples were collected from all sites using precleaned plastic bottles (2 × 1 L for each site). The samples were subsequently transported to laboratory for determination of the elements in the total, total dissolved (< 0.45 µm) and truly dissolved (< 1 kDa) fractions. Amber glass bottles (60 mL) were used to store samples to analyse the content of dissolved organic carbon (DOC) at each site. Samples for DOC were filtered through 0.45 µm membranes and preserved with phosphoric acid (H_3PO_4). All samples were stored at 4°C until analysis.

2.2. Filtration, ultrafiltration and acid digestion

300 mL of the samples were filtered through 0.45 µm cellulose nitrate membranes for determination of the total dissolved fraction of the analysed elements. The truly dissolved

fraction was analysed by further ultrafiltration (UF) of 150 mL through 1 kDa regenerated cellulose membranes (Millipore). The UF was carried out using a Teflon home-made tangential UF system coupled to a Gilson Minipuls® 3 peristaltic pump, similar as described in Monteiro et al. (2016). The system and membranes were cleaned using NaOH (0.1 mol L^{-1}) and HCl (< 0.01 mol L^{-1}) solutions followed by rising with ultrapure water (18.2 MΩ, Millipore) before each filtration.

Acid digestion of the fractions total (not filtered, 150 mL), total dissolved (< 0.45 µm, 150 mL) and truly dissolved (< 1 kDa, 150 mL) followed by a six-fold preconcentration (four-fold for the truly dissolved fraction) was performed to detect elements in lower concentrations. The digestion was carried out on a hot plate based on the method 3005A of the U.S. Environmental Protection Agency (US EPA, 1992). Determination of the elements in all digested fractions were performed by inductively coupled plasma optical emission spectrometry (ICP-OES, Agilent Technologies 700 Series). Limits of detection (LoD) and quantification (LoQ) for the elements analysed by ICP-OES are given in the SI section (Table A.1, Appendix A). Blanks of ultrapure water were used to correct measured concentrations. Particulate fraction (> 0.45 µm) and colloidal fraction (< 0.45 µm and > 1 kDa) were calculated by the difference between total and total dissolved fraction and by the difference between total dissolved and truly dissolved fraction, respectively. All experiments were performed in duplicate. A summary of all fractions cited in this investigation is presented within the supplement (Table A.2, SI).

The recovery for all elements measured (from recovery tests for validation) were in the range of 80-120% as shown in Table A.3 (Appendix A, SI).

2.3. Diffusive gradients in thin films (DGT)

Diffusive gradients in thin films (DGT) units were assembled using piston-type devices acquired from DGT research (Lancaster, UK) for determination of DGT-labile species. Each device contained a 0.45 µm cellulose nitrate membrane, a diffusive gel (agarose crosslinked polyacrylamide) layer, and a biding gel layer. Chelex-100 gel was used as binding gel layer for determination of labile Cd, Cr, Cu, Co, Fe, Mn, Ni, Pb and Zn. Ferrihydrite gel was used as binding gel for determination of labile P. The surface area of the piston-like units exposed to the water was 3.14 cm^2 and the thickness of the of the diffusive gel and the cellulose nitrate membrane were 0.8 mm and 0.13 mm, respectively.

Three DGT units containing chelex-100 gel and three units containing ferrihydrite were deployed at each sampling site. The units were retrieved after 4 to 9 days (cf. Table A.4, Appendix A, SI), rinsed with ultrapure water, stored in plastic bags, and transported to the laboratory. Water temperature was measured *in situ* during deployment and retrieval at each site for determination of the diffusion coefficients of all analysed elements. In laboratory, the DGT units were opened, and the chelex-100 gel layers were eluted with 2 mL of HNO_3 (1 mol L^{-1}). The ferrihydrite gels were eluted with 2 mL of concentrated HCl for 24 h in a shaker and then diluted with ultrapure water.

The concentration of the analysed elements (C_e, µg L^{-1}) after elution was analysed with ICP-OES (Agilent Technologies 700 Series). The accumulated mass of each analyte (M, ng) was subsequently calculated using the following equation (Zhang and Davison, 1995):

$$M = C_e(V_e + V_g)/E_f \quad (1)$$

where V_e is the volume of the eluent (mL), V_g is the volume of the binding gel (mL) and E_f is the elution factor (cf. Table A.4, Appendix A). The DGT-labile concentration of each analyte (C_a, µg L^{-1}) was then calculated using the following equation (Zhang and Davison, 1995):

$$C_a = M\Delta g/DtA \quad (2)$$

where Δg is the thickness of the diffusive gel and cellulose nitrate filter (cm), A is the exposed area to water in the river/stream (cm^2), t is the deployment time (s), and D is the diffusion coefficient (cm^2 s^{-1}). The diffusion coefficients of each element analysed are available from DGT research (https://www.dgtresearch.com, accessed in October 2020; Table A.5, Appendix

A, SI). The coefficients were corrected using the average temperature measured *in situ* during deployment and retrieval of the DGT units (Table A.6, Appendix A, SI).

2.4. Self-organising maps and Spearman's rank correlation

The relationships among samples, variables and between samples and variables were investigated using the SO-Map approach. The SO-Map consists of neurons in a two-dimensional grid. Each input sample in this technique is represented by a vector whose elements correspond to the concentrations of the four fractions (total, total dissolved, truly dissolved, and DGT-labile) of each investigated element (Cd, Cr, Cu, Co, Fe, Mn, Ni, P, Pb and Zn) and the physicochemical parameters (conductivity, TDS, pH and temperature) measured at each sampling site. The neurons in the output map have the same dimension (each one represented by a component plane) of the input vectors. The input and output layers are connected by weight vectors. These vectors are initialised with small random numbers in the analysis. Then, the Euclidean distance between an input vector and the weight vector of each output neuron is calculated. The neuron with the smallest distance (best matching unit, BMU) from the input vector in then selected and the weight vector of the BMU and its neighbours are updated (Çinar and Merdun, 2009; Asan and Ercan, 2012; Brereton, 2012).

The data were normalised before the analysis using z-score transformation for converting the variables to a common scale with mean zero and standard deviation one. Different map architectures (2×2 to 6×6) were tested to find the map with the most informative distribution of the samples. The optimal number of neurons should not be too high or too low because the samples would be respectively too far apart or too close, decreasing the possibility to extract information (Garcia et al., 2007). The software Matlab 2017b (MathWorks, Natick, MA) and the SOM toolbox 2.1 (Alhoniemi et al., 2000) were used to perform the SO-Map analysis.

The correlation between the variables was investigated using Spearman's rank correlation coefficients in the R software. Moderate or strong correlations were expressed by coefficients (ρ) higher than 0.40 (positive correlation) or lower than −0.40 (negative correlation). To run SO-Map and correlation analyses, concentration values of elements measured by ICP-OES below the limit of detection were replaced by these values. The file (.txt) used for running the SO-Map analysis is available in the SI.

3. Results

Sampling site S1 showed the highest concentrations of Mn and P, especially in the dry season (Fig. 2). This site also recorded the highest conductivity (292 µS cm^{-1}), pH (7.2), TDS (194 mg L^{-1}) and the highest concentration of DOC (4.0 mg L^{-1}) in the dry season (Table A.7, Appendix A, SI). In contrast, lowest values of conductivity, TDS, and Mn and P concentrations were observed at S3 and S4. Sites S7 and S9 presented the highest concentrations of Co, Cu and Ni, while S3 showed the highest amounts of Zn. Cd, Cr, and Pb were not detected in most samples (cf. Table A.8, Appendix A). Small amounts (up to 5.7 µg L^{-1}) of total Cr and Pb were detected at sites S1, S6, and S9. DGT-labile Cd (0.12±0.05 µg L^{-1}) and Cr (0.13±0.08 µg L^{-1}) were also detected at site S7 in the rainy season (Fig. 2, Table A.8 within SI).

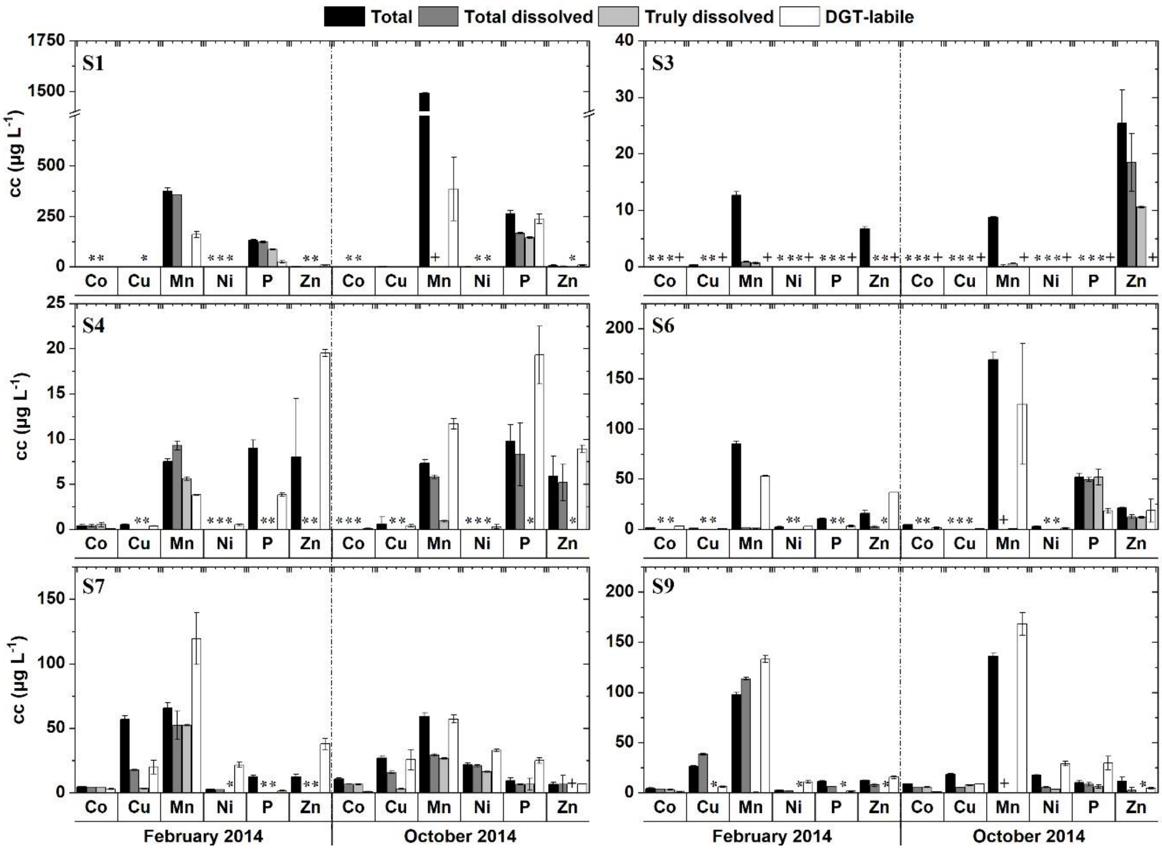

Fig. 2 Concentration (cc) of Co, Cu, Mn, Ni, P and Zn in the total, total dissolved, truly dissolved, and DGT-labile fractions from the six sampling sites (S1, S3, S4, S6, S7 and S9) in Upper Doce River catchment. Not detected and not determined values are depicted as * and +, respectively. These results are available in the Appendix B, supplementary information (SI), tables B.1-B.2.

Regarding the different fractions (Fig. A.2, Appendix A), Co and P occurred predominantly in the truly dissolved fraction (< 1 kDa) in most samples. Mn was predominant in the colloidal fraction at S1 and S9 in the rainy season and at S4 in the dry season, while it was predominant in the truly dissolved fraction at S4 and S7 in the rainy season. Cu occurred mainly in the particulate fraction at sites S1 and S9 in the dry season and at S7 in the rainy season. The highest concentrations of DGT-labile Ni occurred at sites S7 and S9 (33.0±0.9 and 29.1±2.2 µg L^{-1}, Fig 2) and of DGT-labile Cu at S7 (25.8±7.8 µg L^{-1}). Most of total dissolved P was found in the DGT-labile fraction (Fig. 2) and the same behaviour was observed for Mn, except at S1 (rainy season) where only about half of the total dissolved Mn was DGT-labile.

The samples were divided by SO-Map analysis in four (I-IV) distinct groups that are circled in Fig. 3 A. These groups represent samples that have similar properties since they are in the same or neighbouring neurons (hexagonal units). The larger the distance between two samples in the maps, the more dissimilar from each other they are (Garcia et al., 2007). The map architecture 4 × 4 was selected because it gives the best distribution of samples (most informative) in the SO-Map analysis. Behind the map of samples (Fig. 3 A), there are component planes (map of variables, Fig. 3 B) that correspond to the variables used to create the maps (Brereton, 2012).

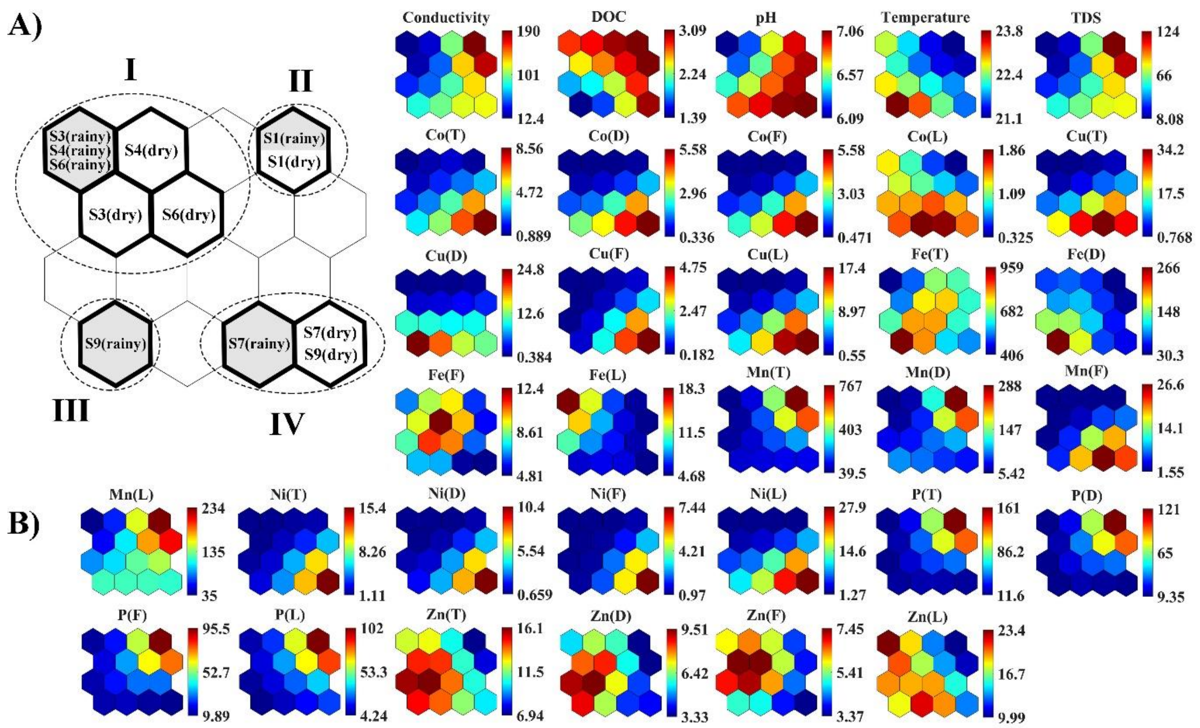

Fig. 3 Self-organising maps: A) Map of samples, in which samples from six sites (S1, S3, S4, S6, S7 and S9) were clustered in four distinct groups (I-IV) as circled in the map. The sampling season (rainy or dry) when water was collected is indicated in parenthesis and by grey (rainy season) and white (dry season) tones in the neurons (hexagonal units). B) Maps of variables (component planes): the bars beside each map indicate the intensity of each variable (red is high intensity and blue is low intensity). The fractions total, total dissolved, truly dissolved, and DGT-labile are indicated by the letters T, D, F and L (in brackets), respectively. The used Fe data were derived from Gontijo et al. (2016).

Group I in the map includes samples with lower conductivity, pH, TDS and lower content of Co, Cu, Mn, Ni, and P (blue colours in the maps of these variables at the corresponding position of group I, Fig. 3 B). The total and total dissolved Fe content in group I is lower than in other groups, but it has samples with the highest truly dissolved and DGT-labile Fe contents (see red colours for these variables at the position of group I, Fig. 3). Group II is formed by S1 samples which exhibit the highest conductivity, DOC, TDS and highest Mn and P contents. Water temperature and concentrations of all other measured elements were low in this second group. Group IV (samples from S7 and S9) had samples with higher amounts of Cu and Ni. The sample taken at S9 in the rainy season formed a separated group out from other samples at S9 because of its higher concentrations of total and total dissolved Fe and Zn. A summary of the most relevant variables for each group is presented in the supplementary section (Table A.9, Appendix A).

The analysis of the map of variables (Fig. 3 B) can also indicate correlations between variables. These correlations are revealed when there are similar or opposite patterns at the same positions in the neurons of a pair of maps of variables (Vesanto, 1999). Neurons with higher intensity for total dissolved Fe (red tones, Fig. 3 B) for instance have lower intensity for P fractions (blue tones), indicating inverse relationship between these P-fractions and total dissolved Fe. In fact, a negative correlation (−0.55, p=0.10; Table A.10, Appendix A) was confirmed between total dissolved Fe and DGT-labile P. A positive relationship is observed among the variables conductivity, DOC, TDS, total Mn, total dissolved Mn, DGT-labile Mn, total P, total dissolved P, truly dissolved P, and DGT-labile P, since all these variables presented red tones in the corresponding neurons in the maps (note that the maps of these variables are similar to each other, Fig. 3 B). Significant ($p < 0.05$) positive correlations were confirmed for example between total P and conductivity/TDS (both 0.75), total Mn and conductivity/TDS (0.78 and 0.79, respectively) and DOC and labile P (0.65). Similar patterns in the maps can also be observed between Co, Cu and Ni fractions, confirmed by positive correlations (up to 0.95) between total Ni and Co.

4. Discussion

4.1. Species distribution, potential bioavailability and seasonality

The high P contents (up to 263±16 μg L^{-1}) in samples from Carmo River (site S1, samples from group II, Fig. 3) are probably related to untreated urban sewage effluent discharge, which is a problem already reported in the literature (Santos et al., 2019). The higher conductivity, DOC and TDS also support this assumption because these variables are also related to sewage inputs in rivers (Daniel et al., 2002). P concentration was lower during the rainy season (Fig. 2), probably because of dilution of the sewage effluent by higher river flow as a result of increased precipitation in the summer period (cf. Fig. A.3, Fig. A.4, Appendix A).

P appeared predominantly in the truly dissolved fraction and is mostly DGT-labile at all sampling sites. These DGT-labile species include species that dissociate and/or desorb in the medium, diffusing through the gel layer and accumulating in the binding gel during the deployment time (Zhang and Davison, 1995; Zhang and Davison, 2015). Although different organisms have different uptake mechanisms, the labile species measured by DGT are considered potentially bioavailable (Zhang and Davison, 2015). Therefore, higher concentrations of DGT-labile and potentially bioavailable P at S1 and S6 may cause cyanobacteria blooms which have been already recorded downstream in Doce River catchment and correlated to total P, particularly in the dry season (Jardim et al., 2014). The data also indicated that the presence of total dissolved Fe may decrease the amount of DGT-labile P (negative correlation), probably because P tends to bind effectively to Fe colloids (e.g. Fe-oxyhydroxides and Fe-organic matter) that are not labile and may be not readily bioavailable to biota (Eisenreich and Armstrong, 1980; Baken et al., 2014; Baken et al., 2016; Gontijo et al., 2016). The positive correlation (0.68) between total Fe and total P may also be related to the P binding of Fe.

The highest measured Mn content was also detected at S1, where it may be derived from manganese-bearing rocks in the banded iron formation of the Quadrilatero Ferrífero (Dorr, 1969; Costa et al., 2003). Mobilisation from old gold and manganese exploitation may have contributed to increase the amounts of Mn in Carmo River (Costa et al., 2003). Mn appeared predominantly in the particulate and colloidal fractions, except in S7 samples. This colloidal Mn may appear as Mn oxides or bound to humic substances (HS), Fe-rich colloids and other ligands in the aquatic system (Huangfu et al., 2013; Li et al., 2019).

The sampling sites S3, S4 and S6 (group I, Fig. 3) showed the best water quality by lowest concentrations of all elements analysed, except Zn at S3 and S6. Measurements of DOC at the retrieval time of DGT devices at S4 showed a DOC increase from 4.7±0.1 to 9.0±0.1 mg L^{-1} (Table A.13, Appendix A) after several days of strong rainfall (72.8 mm between 15 and 19th February 2014, Table A.11; see also Table A.12, Appendix A). This increase of DOC was associated with a drop in pH down to 4.4 and it is related to the presence of HS (Gontijo et al., 2016; Gontijo et al., 2017b). Higher contents of HS at S4 after rainfalls may impact the species distribution in the rivers from Upper Doce River catchment because HS stabilise for instance Fe in the colloidal fraction, thereby increasing its mobility (Ritter et al., 2006). A greater presence of Fe complexed to HS can also affect the distribution of P in the catchment, moving it from the truly dissolved to the colloidal fraction by binding to the complexed Fe (Ritter et al., 2006; Gontijo et al., 2017b; Saeed et al., 2018).

The samples from Conceição River (particularly at S9) are the ones (groups III and IV, Fig. 3) where seasonality was detected using SO-Map analysis (samples are in different groups). This difference was caused especially by higher Fe and lower Ni and Co content in the rainy season than in the dry season. The higher Fe content may be attributed to the leaching of soils due to rainfall during the rainy season (cf. annual precipitation in the area in Fig. A.3, Appendix

A). Conversely, Ni and Co are diluted in the rainy season because of higher water flow of the river. Ni may be derived from ultramafic rocks or laterite ores present in the area (Terezinha Costa et al., 2006). Co may also appear in laterite ores as substitute of Fe and its high correlation with Ni (0.95, $p < 0.05$) supports the natural origin (Ribeiro et al., 2020). Most of the total dissolved Zn was DGT-labile and consequently potentially bioavailable. The DGT-lability of both, Cu and Zn decreased from S7 to S9 in the Conceição River. This may be connected to the input of HS from Caraça River catchment (Gontijo et al., 2016) that can bind these elements, reducing their lability (McKnight et al., 1983; Chakraborty and Chakrabarti, 2008).

The trace-metals Cd, Cr, and Pb were not detected in most samples. Cr and Pb were found in samples from Carmo and Conceição rivers mostly in the total fraction which may be related to resuspension from sediments where they have already been recorded (Deschamps et al., 2002; Terezinha Costa et al., 2006; Marques et al., 2019). DGT-labile Cd was found at S7 (0.12 ± 0.05 µg L^{-1} Cd), probably due to the pre-concentration capabilities of DGT (Zhang and Davison, 1995).

Table A.14 (Appendix A) presents the total dissolved concentrations of the analysed elements (without digestion) at the retrieval time in October/2014. It shows that the concentrations of most of the detected elements were quite similar to the ones from the deployment time (Fig. 2) in the dry season, except for Cu at S7. This difference reflects the dynamic environment with presence of several processes such as the ones described above in a way that aquatic systems are hardly at chemical equilibrium (van Leeuwen et al., 2005).

4.2. Legislation and possible effects of the dam collapse

The Brazilian National Environmental Council (CONAMA), in its Resolution 357/2005 (Brazil, 2005), established regulations and guidelines for the classification of water bodies according to their intended use. There are several classes in which water quality standards are assigned and must be preserved. The waters from Doce River catchment are classified as Class

2, in which the use is intended for protection of aquatic life, water supply after conventional treatment, recreation, fishing and irrigation (IGAM, 2015). Several parameters in the samples from Upper Doce River catchment were above the limits of class 2, especially in Carmo and Conceição rivers. Total P and Mn concentrations at S1 for instance were much higher (up to 263 µg L^{-1} P and up to 1491 µg L^{-1} Mn) than the standards for class 2 (100 µg L^{-1} for both P and Mn, Table A.15, Appendix A). Besides total Mn, samples from Conceição River (at S7 and S9) had also higher values for total dissolved Cu (max. 38.5 µg L^{-1} Cu) than the limit by legislation (9 µg L^{-1} Cu). These results shows that the water quality in the studied area was already impaired by natural and human factors, even before the dam breach at Mariana in 2015.

From literature it is known that the dam burst in the investigated area has initially caused an increase in the amount of suspended particulate matter (SPM) and turbidity in the river waters. That derived from the sludge and mud and was composed mainly of Fe and Si oxides (Pires et al., 2003; IBAMA, 2015; IGAM, 2015; Fraga et al., 2021). This material was transported downstream and stored in riverbeds and flood plains after most of the tailings from the accident was settled. According to Hatje et al. (2017), heavy rainfall may contribute to further erosion and remobilisation of the deposited material in the future. Such events may change the distribution and bioavailability of some elements in the affected systems. P for example was mostly present in the truly dissolved fraction but it will probably bind to increasing contents of Fe-rich particulate matter, thereby transferring it from the truly dissolved to the particulate fraction (Smith and Longmore, 1980). This change of distribution subsequently will affect the mobility and lability of the elements in the water column and may also impact for example the levels of chlorophyll-a and trophic status in some reservoirs along Doce River (Coimbra et al., 2020).

Comparing total and total dissolved metal contents analysed after the accident (Hatje et al., 2017; IGAM, 2018; Silva et al., 2018; Foesch et al., 2020, Table A16, Appendix A) with the results from our study, higher Cr, Cu, Fe, Pb, and Mn contents were observed in Carmo

River and Ouro Fino Stream after the accident. The concentration of total Mn in Carmo River for instance was much higher after the accident (up to 13400 μg L^{-1} Mn in 2015; IGAM, 2018) than before (up to 1491 μg L^{-1} Mn in this study). The total dissolved Mn in Ouro Fino Stream was also higher after the accident (117 μg L^{-1} Mn, Hatje et al. (2017)) than before (up to 0.9 μg L^{-1} Mn in this study). Total Pb which was not detected in Carmo River in this investigation reached values above 40 μg L^{-1} in 2015 and 2016 (IGAM, 2018; Foesch et al., 2020), exceeding the Brazilian limit of Pb for class 2 freshwaters (Table A.15, Appendix A). Total dissolved Fe and total Cu contents in Carmo River also presented an expressive increase, from maximum of 9 μg L^{-1} Fe and 2 μg L^{-1} Cu in this study to 2620 μg L^{-1} Fe and 20 μg L^{-1} Cu after the accident (Hatje et al., 2017; IGAM, 2018; Foesch et al., 2020), respectively. However, there is still no information regarding species distribution and DGT-lability in the water column after the dam collapse in the area for comparison and impact evaluation.

5. Conclusions

Both techniques (DGT and ultrafiltration) were complementary used to study the distribution and DGT-lability of P and some trace elements within the upper Rio Doce catchment affected by mining (e.g., aluminium, iron, gold and manganese). Our results show that even under "natural" background conditions before the dam failure of Mariana in 2015, the element concentrations of some trace metals and phosphorus were in part above the Brazilian limits for freshwater class 2 due to natural and anthropogenic factors such as local lithology (Mn, Cu, Ni, Co), mining (Cu, Zn, Pb) and untreated sewage discharge (P, DOC).

Carmo River exhibited the highest P concentrations, which occurred predominantly in the truly dissolved and DGT-labile fractions, indicating that it is mobile and potentially bioavailable. The data indicated that Fe may have decreased the amount of DGT-labile P by adsorption processes to increase the particulate amount of P. Cd was detected only in the DGT-labile fraction but not in the fractions measured by filtration and ultrafiltration because of the pre-concentration capabilities of DGT. The DGT-labile amount of Cu and Zn decreased over the investigated stretch of the Conceição River, indicating the presence of other ligands (e.g., HS) and/or particles (> 0.45 µm) in the water phase which is supported by a contemporaneous increase of the colloidal and/or particulate concentrations. Effects of seasonality (dry vs. rainy seasons) were detected only in Conceição River and was attributed especially to Fe, Ni and Co. Concentrations of Ni and Co were lower in the wet season than in the dry season due to the dilution effect. In contrast, the concentrations of Fe increased in the rainy season, presumably due to increased erosion of lateritic soils.

The dam burst in the catchment with the subsequent increase in particulate material deposited downstream in the riverbed and floodplains has the potential to affect the aquatic life in the catchment. To assess the ecological impacts and fate of the dam failure of Mariana in 2015, a continuous chemical monitoring including the distribution and DGT-lability of trace-metals and nutrients would be mandatory. Our study provides a basis for such monitoring and allows comparison of post-accident chemical exposure with "quasi-natural" background concentration ranges of the situation before the dam failure.

Acknowledgments

We are thankful to the Graduate Program in Environmental Engineering (ProAmb) from the Federal University of Ouro Preto (UFOP) that provided infrastructure for some analysis and the field trips. We grateful acknowledge the help of Ms. Deyse Reis, Mr. Edilson Oliveira and Ms. Laura Nascimento for their support in field and laboratory.

Declarations

Ethics approval and consent to participate

Not applicable

Consent for publication

Not applicable

Research data

All data generated or analysed during this study are included in this published article [and its supplementary information files]. They can also be accessed at https://data.mendeley.com/datasets/6bwcgxsrkx/2.

Funding

This research was supported by the São Paulo Research Foundation (FAPESP, grant numbers 12/17727-8, 13/14122-0 and 19/06800-5), the German Academic Exchange Service (DAAD, grant number DAAD- ID 57414997) and the Brazilian Coordination for the Improvement of Higher Education (CAPES, grant numbers BEX10452/14-1 via CAPES/DAAD scholarship program and 99999.008107/2015- 07).

Supplementary Information (SI)

Supplementary files to this article including appendices A and B can be found online.

References

Alhoniemi, E., Himberg, J., Parhankangas, J., Vesanto, J., 2000. SOM Toolbox.

Allen, H.E., Hansen, D.J., 1996. The importance of trace metal speciation to water quality criteria. Water Environ. Res 68, 42-54. https://doi.org/10.2175/106143096X127307.

Asan, U., Ercan, S., 2012. An Introduction to Self-Organizing Maps. in: Kahraman, C. (Ed.). Computational Intelligence Systems in Industrial Engineering: With Recent Theory and Applications. Atlantis Press, Paris, pp. 295-315.

Baken, S., Moens, C., van der Grift, B., Smolders, E., 2016. Phosphate binding by natural iron-rich colloids in streams. Water Res. 98, 326-333. https://doi.org/10.1016/j.watres.2016.04.032.

Baken, S., Nawara, S., Van Moorleghem, C., Smolders, E., 2014. Iron colloids reduce the bioavailability of phosphorus to the green alga Raphidocelis subcapitata. Water Res. 59, 198-206. https://doi.org/10.1016/j.watres.2014.04.010.

Brereton, R.G., 2012. Self organising maps for visualising and modelling. Chemistry Central Journal 6, S1. https://doi.org/10.1186/1752-153X-6-S2-S1.

Buffle, J., 1991. Complexation Reactions in Aquatic Systems: An Analytical Approach. Ellis Horwood Ltd.

Carmo, F.F.d., Kamino, L.H.Y., Junior, R.T., Campos, I.C.d., Carmo, F.F.d., Silvino, G., Castro, K.J.d.S.X.d., Mauro, M.L., Rodrigues, N.U.A., Miranda, M.P.d.S., Pinto, C.E.F., 2017. Fundão tailings dam failures: the environment tragedy of the largest technological disaster of Brazilian mining in global context. Perspectives in Ecology and Conservation 15, 145-151. https://doi.org/10.1016/j.pecon.2017.06.002.

Chakraborty, P., Chakrabarti, C.L., 2008. Competition from Cu(II), Zn(II) and Cd(II) in Pb(II) Binding to Suwannee River Fulvic Acid. Water, Air, and Soil Pollution 195, 63-71. https://doi.org/10.1007/s11270-008-9727-7.

Çinar, O., Merdun, H., 2009. Application of an unsupervised artificial neural network technique to multivariant surface water quality data. Ecological Research 24, 163-173. https://doi.org/10.1007/s11284-008-0495-z.

Coimbra, K.T.O., Alcântara, E., de Souza Filho, C.R., 2020. Satellite evidence for pervasive water eutrophication in the Doce River reservoirs following the collapse of the Fundao dam in Brazil. Environmental Pollution, 116014. https://doi.org/10.1016/j.envpol.2020.116014.

Costa, A.T., Nalini, H.A., de Lena, J.C., Friese, K., Mages, M., 2003. Surface water quality and sediment geochemistry in the Gualaxo do Norte basin, eastern Quadrilátero Ferrífero, Minas Gerais, Brazil. Environ. Geol. 45, 226-235. https://doi.org/10.1007/s00254-003-0870-6.

Daniel, M.H.B., Montebelo, A.A., Bernardes, M.C., Ometto, J.P.H.B., Camargo, P.B.d., Krusche, A.V., Ballester, M.V., Victoria, R.L., Martinelli, L.A., 2002. Effects of Urban Sewage on Dissolved Oxygen, Dissolved Inorganic and Organic Carbon, and Electrical Conductivity of Small Streams along a Gradient of Urbanization in the Piracicaba River Basin. Water, Air, and Soil Pollution 136, 189-206. https://doi.org/10.1023/A:1015287708170.

Davison, W., Zhang, H., 1994. In situ speciation measurements of trace components in natural waters using thin-film gels. Nature 367, 546-548. https://doi.org/10.1038/367546a0.

Deschamps, E., Ciminelli, V., Lange, F., Matschullat, J., Raue, B., Schmidt, H., 2002. Soil and sediment geochemistry of the iron quadrangle, Brazil the case of arsenic. Journal of Soils and Sediments 2, 216-222. https://doi.org/10.1007/bf02991043.

Dorr, J.V.N., 1969. Physiographic, Stratigraphic and Structural Development of the Quadrilátero Ferrífero, Minas Gerais, Brazil: Regional Geology of the Quadrilátero Ferrífero, Minas Gerais, Brazil. Regional geology of the Quadrilatero Ferrifero, Minas Gerais, Brazil, 110.

Eisenreich, S.J., Armstrong, D.E., 1980. Association of organic matter, iron and inorganic phosphorus in lake waters. Environment International 3, 485-490. https://doi.org/10.1016/0160-4120(80)90156-7.

Foesch, M.D.S., Francelino, M.R., Rocha, P.A., Gomes, A.R.L., 2020. River Water Contamination Resulting from the Mariana Disaster, Brazil. Floresta e Ambiente 27.

Forsberg, J., Dahlqvist, R., Gelting-Nystrom, J., Ingri, J., 2006. Trace metal speciation in brackish water using diffusive gradients in thin films and ultrafiltration: Comparison of techniques. Environ. Sci. Technol. 40, 3901-3905. https://doi.org/10.1021/es0600781.

Fraga, M.d.S., da Silva, D.D., Reis, G.B., Guedes, H.A.S., Elesbon, A.A.A., 2021. Temporal and spatial trend analysis of surface water quality in the Doce River basin, Minas

Gerais, Brazil. Environment, Development and Sustainability. https://doi.org/10.1007/s10668-020-01160-8.

Garcia, J.S., Da Silva, G.A., Arruda, M.A.Z., Poppi, R.J., 2007. Application of Kohonen neural network to exploratory analyses of synchroton radiation x-ray fluorescence measurements of sunflower metalloproteins. X-Ray Spectrom. 36, 122-129. https://doi.org/10.1002/xrs.950.

Garmo, Ø.A., Lehto, N.J., Zhang, H., Davison, W., Røyset, O., Steinnes, E., 2006. Dynamic Aspects of DGT as Demonstrated by Experiments with Lanthanide Complexes of a Multidentate Ligand. Environ. Sci. Technol. 40, 4754-4760. 10.1021/es060674v.

Gontijo, E.S.J., Herzsprung, P., Lechtenfeld, O.J., de Castro Bueno, C., A.C. Barth, J., Rosa, A.H., Friese, K., 2021. Multi-proxy approach involving ultrahigh resolution mass spectrometry and self-organising maps to investigate the origin and quality of sedimentary organic matter across a subtropical reservoir. Org. Geochem. 151, 104165. https://doi.org/10.1016/j.orggeochem.2020.104165.

Gontijo, E.S.J., Monteiro, A.S.C., Rosa, A.H., 2017a. Metal and Metalloid Speciation in Aquatic Environments: Concepts, Techniques and Applications. Revista Virtual de Química 9, 1910-1929. https://doi.org/10.21577/1984-6835.20170112.

Gontijo, E.S.J., Watanabe, C.H., Monteiro, A.S.C., da Silva, G.A., Roeser, H.M.P., Rosa, A.H., Friese, K., 2017b. Effects of Fe(III) and quality of humic substances on As(V) distribution in freshwater: Use of ultrafiltration and Kohonen neural network. Chemosphere 188, 208-217. https://doi.org/10.1016/j.chemosphere.2017.08.143.

Gontijo, E.S.J., Watanabe, C.H., Monteiro, A.S.C., Tonello, P.S., da Silva, G.A., Friese, K., Roeser, H.M.P., Rosa, A.H., 2016. Distribution and bioavailability of arsenic in natural waters of a mining area studied by ultrafiltration and diffusive gradients in thin films. Chemosphere 164, 290-298. http://dx.doi.org/10.1016/j.chemosphere.2016.08.107.

Hatje, V., Pedreira, R.M.A., de Rezende, C.E., Schettini, C.A.F., de Souza, G.C., Marin, D.C., Hackspacher, P.C., 2017. The environmental impacts of one of the largest tailing dam failures worldwide. Scientific Reports 7, 10706. https://doi.org/10.1038/s41598-017-11143-x.

Huangfu, X., Jiang, J., Ma, J., Liu, Y., Yang, J., 2013. Aggregation Kinetics of Manganese Dioxide Colloids in Aqueous Solution: Influence of Humic Substances and Biomacromolecules. Environ. Sci. Technol. 47, 10285-10292. https://doi.org/10.1021/es4003247.

IBAMA, 2015. Lauto Técnico Preliminar: Impactos Ambientais Decorrentes do Desastre Envolvendo o Rompimento da Barragem de Fundão, em Mariana, Minas Gerais., 38 p.

IGAM, 2015. Acompanhamento da Qualidade das Águas do Rio Doce Após o Rompimento da Barragem da Samarco no distrito de Bento Rodrigues – Mariana/MG. Monitoramento da Qualidade das Águas Superficiais do Rio Doce no Estado de Minas Gerais. Minas Gerais, Brazil, 66 p.

IGAM, 2018. Acompanhamento da Qualidade das Águas do Rio Doce Após o Rompimento da Barragem da Samarco no distrito de Bento Rodrigues – Mariana/MG. Monitoramento da Qualidade das Águas Superficiais do Rio Doce no Estado de Minas Gerais. Minas Gerais, Brazil.

Jardim, F.A., Sperling, E.v., Jardim, B.F.d.M., Almeida, K.C.d.B., 2014. Fatores determinantes das florações de cianobactérias na água do Rio Doce, Minas Gerais, Brasil. Engenharia Sanitaria e Ambiental 19, 207-218.

Kohonen, T., 2001. Self-Organizing Maps. Springer Berlin Heidelberg.

Li, Q., Xie, L., Jiang, Y., Fortner, J.D., Yu, K., Liao, P., Liu, C., 2019. Formation and stability of NOM-Mn(III) colloids in aquatic environments. Water Res. 149, 190-201. https://doi.org/10.1016/j.watres.2018.10.094.

Marques, L.d.S., Reis, D.A.d., Nascimento, L.P.d., Oliveira, E.G., Santiago, A.d.F., Roeser, H.M.P., 2019. Mobility of metals in river sediments from a watershed in the Iron Quadrangle, Brazil. Geochimica Brasiliensis 33, 273-285. https://doi.org/10.21715/GB2358-2812.2019333273.

McKnight, D.M., Feder, G.L., Thurman, E.M., Wershaw, R.L., Westall, J.C., 1983. Complexation of copper by aquatic humic substances from different environments. Sci. Total Environ. 28, 65-76. https://doi.org/10.1016/S0048-9697(83)80008-4.

Monteiro, A.S.C., Parat, C., Rosa, A.H., Pinheiro, J.P., 2016. Towards field trace metal speciation using electroanalytical techniques and tangential ultrafiltration. Talanta 152, 112-118. http://dx.doi.org/10.1016/j.talanta.2016.01.053.

Morel, F.M.M., 1983. Principles of Aquatic Chemistry. Wiley, New York, NY, USA.

Pires, J.M.M., Lena, J.C.d., Machado, C.C., Pereira, R.S., 2003. Potencial poluidor de resíduo sólido da Samarco Mineração: estudo de caso da barragem de Germano. Revista Árvore 27, 393-397.

Ribeiro, P.P.M., de Souza, L.C.M., Neumann, R., dos Santos, I.D., Dutra, A.J.B., 2020. Nickel and cobalt losses from laterite ore after the sulfation-roasting-leaching processing. Journal of Materials Research and Technology 9, 12404-12415. https://doi.org/10.1016/j.jmrt.2020.08.082.

Ritter, K., Aiken, G.R., Ranville, J.F., Bauer, M., Macalady, D.L., 2006. Evidence for the aquatic binding of arsenate by natural organic matter-suspended Fe(III). Environ. Sci. Technol. 40, 5380-5387. https://doi.org/10.1021/es0519334.

Rodrigues, A.S.d.L., Malafaia, G., Costa, A.T., Nalini Júnior, H.A., 2014. Iron ore mining promotes iron enrichment in sediments of the Gualaxo do Norte River basin, Minas Gerais State, Brazil. Environmental Earth Sciences 71, 4177-4186. https://doi.org/10.1007/s12665-013-2808-y.

Roeser, H.M.P., Roeser, P.A., 2010. O Quadrilátero Ferrífero - MG, Brasil: Aspectos sobre sua história, seus recursos minerais e problemas ambientais relacionados. Geonomos 18, 34-37.

Rougerie, J., Martins de Barros, R., Buzier, R., Devillers, D., Fondanèche, P., Lissalde, S., Leblanc, J., Saüt, M., Rebillard, J.-P., Mazzella, N., Guibaud, G., 2021. Diffusive gradients in thin films (DGT): A suitable tool for metals/metalloids monitoring in continental waterbodies at the large network scale. Sci. Total Environ. 754, 142147. https://doi.org/10.1016/j.scitotenv.2020.142147.

Saeed, H., Hartland, A., Lehto, N.J., Baalousha, M., Sikder, M., Sandwell, D., Mucalo, M., Hamilton, D.P., 2018. Regulation of phosphorus bioavailability by iron nanoparticles in a monomictic lake. Scientific reports 8, 17736-17736. https://doi.org/10.1038/s41598-018-36103-x.

Sans-Duñó, J., Cecilia, J., Galceran, J., Puy, J., 2021. Availability of metals to DGT devices with different configurations. The case of sequential Ni complexation. Sci. Total Environ. 779, 146277. https://doi.org/10.1016/j.scitotenv.2021.146277.

Santamarina, J.C., Torres-Cruz, L.A., Bachus, R.C., 2019. Why coal ash and tailings dam disasters occur. Science 364, 526-528. https://doi.org/10.1126/science.aax1927.

Santos, O.S.H., Avellar, F.C., Alves, M., Trindade, R.C., Menezes, M.B., Ferreira, M.C., França, G.S., Cordeiro, J., Sobreira, F.G., Yoshida, I.M., Moura, P.M., Baptista, M.B., Scotti, M.R., 2019. Understanding the Environmental Impact of a Mine Dam Rupture in Brazil: Prospects for Remediation. Journal of Environmental Quality 48, 439-449. https://doi.org/10.2134/jeq2018.04.0168.

Silva, D.d.C., Bellato, C.R., Marques Neto, J.d.O., Fontes, M.P.F., 2018. Trace Elements in River Waters and Sediments Before and After a Mining Dam Breach (Bento Rodrigues, Brazil). Química Nova 41, 857-866.

Singhal, R.K., Preetha, J., Karpe, R., Tirumalesh, K., Kumar, S.C., Hegde, A.G., 2006. The use of ultra filtration in trace metal speciation studies in sea water. Environment International 32, 224-228. https://doi.org/10.1016/j.envint.2005.08.015.

Smith, J.D., Longmore, A.R., 1980. Behaviour of phosphate in estuarine water. Nature 287, 532-534. https://doi.org/10.1038/287532a0.

Terezinha Costa, A., Arias Nalini Jr., H., de Tarso Amorim Castro, P., Carvalho de Lena, J., Morgenstern, P., Friese, K., 2006. Sediment contamination in floodplains and alluvial terraces as an historical record of gold exploitation in the Carmo River basin, Southeast Quadrilátero Ferrífero, Minas Gerais, Brazil. Acta Hydroch. Hydrob. 34, 245-256. https://doi.org/10.1002/aheh.200400625.

Tonello, P.S., Rosa, A.H., Abreu Jr, C.H., Menegário, A.A., 2007. Use of diffusive gradients in thin films and tangential flow ultrafiltration for fractionation of Al(III) and Cu(II) in organic-rich river waters. Anal. Chim. Acta 598, 162-168. http://dx.doi.org/10.1016/j.aca.2007.07.013.

US EPA, 1992. Method 3005A: Acid Digestion of Waters for Total Recoverable or Dissolved Metals for Analysis by Flaa or ICP Spectroscopy. 5 p.

van Leeuwen, H.P., Jansen, S., 2005. Dynamic aspects of metal speciation by competitive ligand exchange–adsorptive stripping voltammetry (CLE–AdSV). Journal of Electroanalytical Chemistry 579, 337-342. https://doi.org/10.1016/j.jelechem.2005.03.006.

van Leeuwen, H.P., Town, R.M., Buffle, J., Cleven, R.F.M.J., Davison, W., Puy, J., van Riemsdijk, W.H., Sigg, L., 2005. Dynamic Speciation Analysis and Bioavailability of Metals in Aquatic Systems. Environ. Sci. Technol. 39, 8545-8556. https://doi.org/10.1021/es050404x.

Varcjao, E.V.V., Bellato, C.R., Fontes, M.P.F., Mello, J.W.V., 2011. Arsenic and trace metals in river water and sediments from the southeast portion of the Iron Quadrangle, Brazil. Environ. Monit. Assess. 172, 631-642. https://doi.org/10.1007/s10661-010-1361-3.

Vergilio, C.d.S., Lacerda, D., Oliveira, B.C.V.d., Sartori, E., Campos, G.M., Pereira, A.L.d.S., Aguiar, D.B.d., Souza, T.d.S., Almeida, M.G.d., Thompson, F., Rezende, C.E.d., 2020. Metal concentrations and biological effects from one of the largest mining disasters in the world (Brumadinho, Minas Gerais, Brazil). Scientific Reports 10, 5936. https://doi.org/10.1038/s41598-020-62700-w.

Vesanto, J., 1999. SOM-based data visualization methods. Intelligent Data Analysis 3, 111-126. https://doi.org/10.1016/S1088-467X(99)00013-X.

Wen, L.-S., Santschi, P.H., Gill, G.A., Paternostro, C.L., Lehman, R.D., 1997. Colloidal and Particulate Silver in River and Estuarine Waters of Texas. Environ. Sci. Technol. 31, 723-731. https://doi.org10.1021/es9603057.

Zhang, H., Davison, W., 1995. Performance Characteristics of Diffusion Gradients in Thin Films for the in Situ Measurement of Trace Metals in Aqueous Solution. Anal. Chem. 67, 3391-3400. https://doi.org10.1021/ac00115a005.

Zhang, H., Davison, W., 2015. Use of diffusive gradients in thin-films for studies of chemical speciation and bioavailability. Environmental chemistry (Online) 12, 85-101. https://doi.org10.1071/EN14105.

Figure captions

Fig. 1 Sampling sites (S1, S3, S4, S6, S7 and S9), mining areas and tailing dams in Upper Doce River catchment (in Quadrilátero Ferrífero, QF). Mining areas and tailing dams were delineated using cloud-free Landsat 8 imagens taken from path 217 and row 74 on 11th October and 12th November 2015. The images were acquired from the U.S. Geological Survey (USGS) Earth Explorer webpage (https://earthexplorer.usgs.gov/, accessed in December 2020). All delineations were performed using the software ArcGis 10.5 (ESRI, USA).

Fig. 2 Concentration (cc) of Co, Cu, Mn, Ni, P and Zn in the total, total dissolved, truly dissolved, and DGT-labile fractions from the six sampling sites (S1, S3, S4, S6, S7 and S9) in Upper Doce River catchment. Not detected and not determined values are depicted as * and +, respectively. These results are available in the Appendix B, supplementary information (SI), tables B.1-B.2.

Fig. 3 Self-organising maps: A) Map of samples, in which samples from six sites (S1, S3, S4, S6, S7 and S9) were clustered in four distinct groups (I-IV) as circled in the map. The sampling season (rainy or dry) when water was collected is indicated in parenthesis and by grey (rainy season) and white (dry season) tones in the neurons (hexagonal units). B) Maps of variables (component planes): the bars beside each map indicate the intensity of each variable (red is high intensity and blue is low intensity). The fractions total, total dissolved, truly dissolved, and DGT-labile are indicated by the letters T, D, F and L (in brackets), respectively. The used Fe data were derived from Gontijo et al. (2016).

Fig. 1

Click here to access/download;Figure;Fig.1.jpg

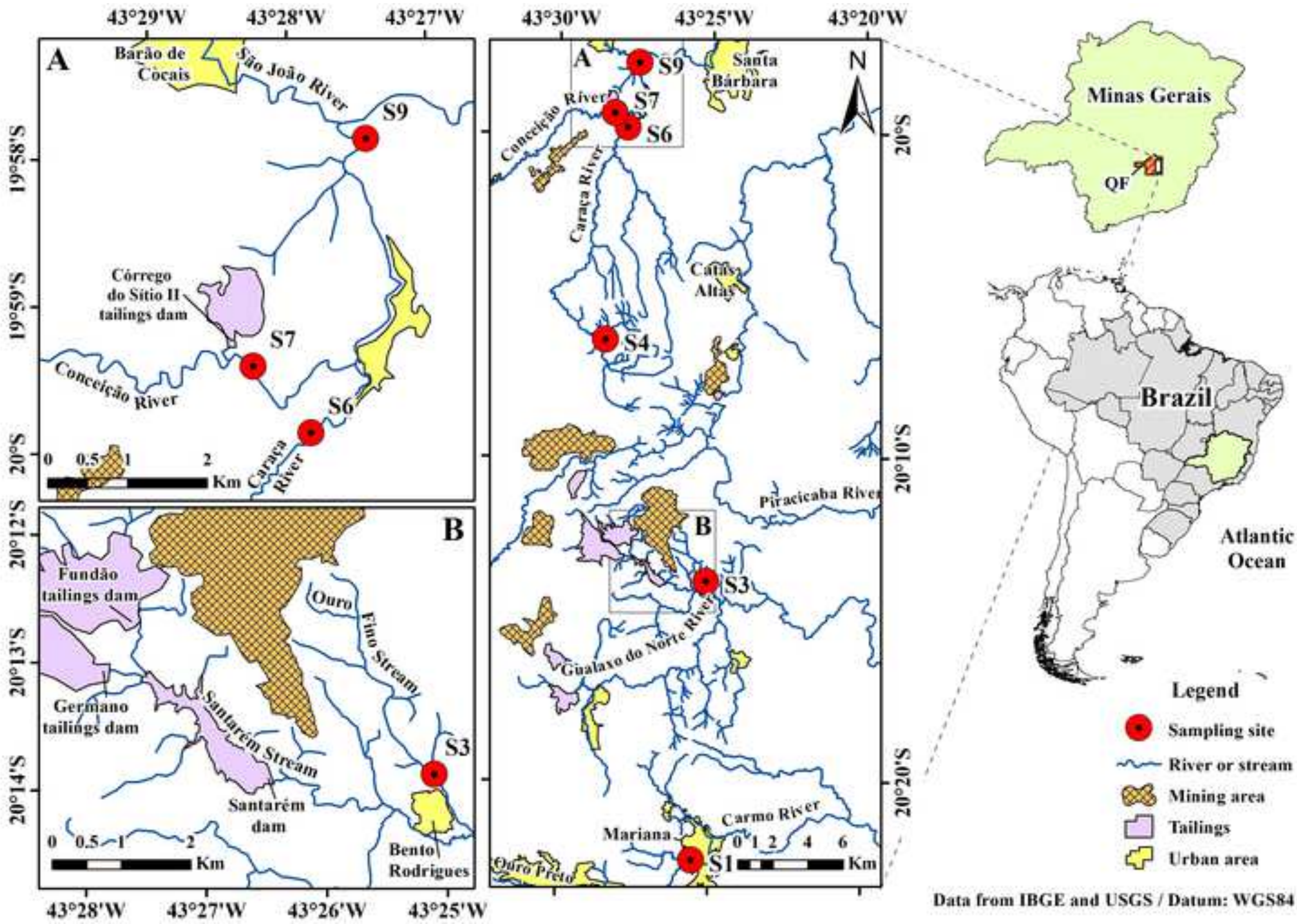

Fig. 2

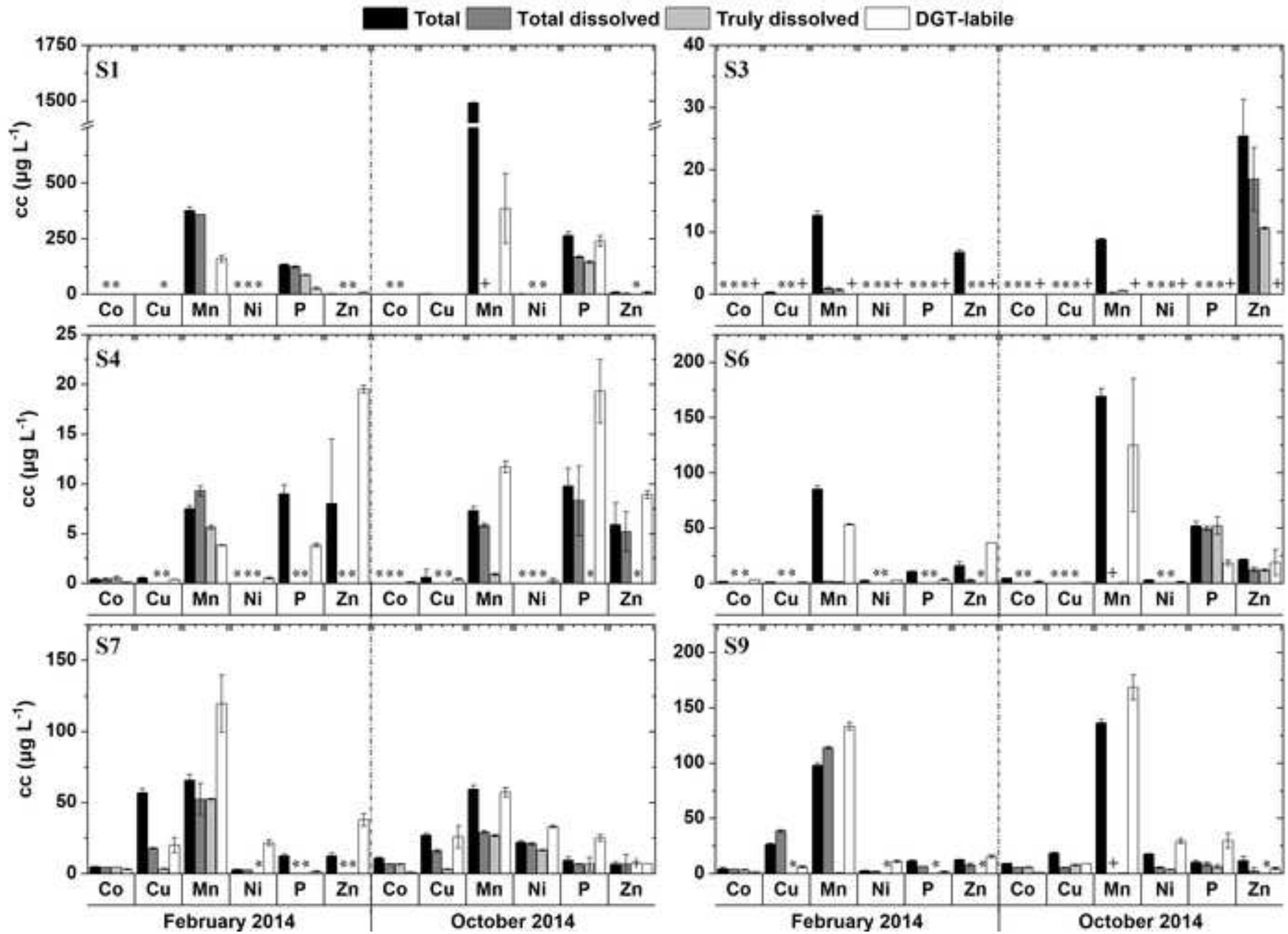
Total
Total dissolved
Truly dissolved
DGT-labile
S1
S3
S4
S6
S7
S9
cc (µg L-1)
Co
Cu
Mn
Ni
P
Zn
February 2014
October 2014

Fig. 3

Click here to access/download;Figure;Fig.3.jpg